Dry Jet-Wet Spinning of Bagasse/*N*-methylmorpholine-*N*-oxide Hydrate Solution and Physical Properties of Lyocell Fibres

Atsushi Yamamoto,[1] Ahmed Jalal Uddin,[1] Yasuo Gotoh,[1] Masanobu Nagura,[1] Mahito Iwata[2]

[1]*Faculty of Textile Science and Technology, Shinshu University, Ueda, Nagano 386-8567, Japan*
[2]*Division of Chemistry and Materials, Shinnaigai Textile Ltd., Chuo-ku, Osaka 541-0051, Japan*

Received 8 October 2009; accepted 14 February 2010
DOI 10.1002/app.33151
Published online 24 September 2010 in Wiley Online Library (wileyonlinelibrary.com).

ABSTRACT: Sugarcane bagasse, a cheap cellulosic waste material, was investigated as a raw material for producing lyocell fibers at a reduced cost. In this study, bagasse was dissolved in *N*-methylmorpholine-*N*-oxide (NMMO) 0.9 hydrate, and fibers were prepared by the dry jet-wet spinning method with coagulation in an aqueous NMMO solution. The effects of NMMO in 0 to 50% concentrations on the physical properties of fibers were investigated. The coagulating bath contained water/NMMO (10%) solution produced fiber with the highest drawability and highest physical properties. The cross-section morphology of these fibers reveals fibrillation due to the high degree of crystallinity and high molecular orientation. In the higher NMMO concentrated baths (30 to 50%), the prepared fibers were hollow inside, which could be useful to make highly absorbent materials. The lyocell fibers prepared from bagasse have a tensile strength of 510 MPa, initial modulus of 30 GPa, and dynamic modulus of approximately 41 GPa. These properties are very comparable with those of commercial lyocell fibers. © 2010 Wiley Periodicals, Inc. J Appl Polym Sci 119: 3152–3161, 2011

Key words: lyocell; bagasse; NMMO hydrate; dry-jet wet spinning; physical properties

INTRODUCTION

Cellulose is one of the most abundant natural resources on earth and it is a source of biodegradable and eco-friendly regenerated fibers for both apparel and industrial applications.[1,2]

The history of cellulose with respect to regenerated man-made fibers began in the early 1800s as rayon fibers requiring toxic carbon disulfide treatment.[3,4] Recent technical breakthroughs have solved problem of toxicity by directly dissolving cellulose in *N*-methylmorpholine-*N*-oxide (NMMO) hydrate. Compared with the conventional viscose fiber route, NMMO technology provides a relatively simple, resource-conserving and environmentally friendly method for producing regenerated cellulose fiber. The manufacturing process is designed to recover 99% of the solvent, which minimizes effluent. The solvent itself is nontoxic and the entire effluent is nonhazardous.[5,6]

The cellulose fibers regenerated from NMMO solutions, known by the generic name lyocell,[7] yield fibers with higher wet strength than those produced using earlier technologies.[8–10] Among the different spinning techniques, the dry jet-wet spinning method was found to produce lyocell fibers with good physical properties.[11,12] In addition, dry jet-wet spun lyocell breathes and washes like cotton and shrinks less when wet than other cellulose fibers. Moreover, it has the soft, natural draping qualities of rayon with a luxurious and refined look.

The cellulose of lyocell is usually derived from pulp with high α-cellulose pulp content, as found in hardwood tress such as eucalyptus, oak, and birch. Eucalyptus trees cause invasive water sucking from the ground; therefore, the land becomes unsuitable for food production. In addition, a eucalyptus forest tends to promote fire because of the volatile and highly combustible oils produced by the leaves. Furthermore, the production of pulp material from these trees is relatively costly.[13] Conversely, bagasse is a much cheaper, environmentally friendly pulp that can reduce the cost of lyocell fibers while protecting the environment. Bagasse is derived from the crushing of sugarcane stalks, and it is used in industry to produce power, paper, and building materials such as particleboard, fuel, and even stock feed. However, its annual production of approximately 100 million tons causes mills to incur additional disposal costs, and an excess of bagasse is continually deposited on empty fields, altering the landscape.

The composition of bagasse is 50% cellulose, 30% hemicellulose, 18% lignin, and some inorganic

Correspondence to: Y. Gotoh (ygotohy@shinshu-u.ac.jp).
Contract grant sponsors: Global COE program by the Ministry of Education, Culture, Sports, Science and Technology of Japan.

compounds.[14] Because bagasse contains more than 20% hemicellulose, it is termed a high hemicellulose pulp.[15] Recent investigations report that the yield of lyocell fibers produced from high and low hemicellulose content are almost the same because both cellulose and hemicellulose content are converted into fiber during the lyocell process.[16,17] In addition, higher hemicellulose content was found to be beneficial in forming a smaller fibril aggregation.[18–20] The hemicellulose associated with cellulose can increase the stability of fibril aggregation.[21,22] This fact ultimately restricts fibrillation of lyocell fibers.[23,24]

The main objective of our current research is to prepare lyocell fibers from the raw material of a cheaper source such as sugarcane bagasse. The fibers were prepared according to the conventional lyocell process of dry jet-wet spinning using NMMO hydrate as a solvent and aqueous NMMO solution as a coagulant. Varying NMMO concentrations in the coagulation bath were also investigated to find the coagulation solution generating the best physical properties.

EXPERIMENTAL

Materials

The bagasse used in this study was supplied by Okinawa Sugarcanes Research Corp. in Japan. The bagasse was agitated at 80 rpm and temperature 90°C for 24 h with 10% alkali (NaOH) solution to remove lignin and other inorganic compounds. Elimination of lignin was confirmed by Fourier transform infrared (FTIR) spectra and differential scanning calorimetry (DSC). From the thermogravimetric analysis (TGA) study, a greater portion of inorganic matter was found to be eliminated after treatment of bagasse with 10% NaOH.

A commercial lyocell fiber sample was received from Shinnagai Textile Ltd, Japan for comparison of its mechanical properties with those of our prepared fibers. The NMMO hydrate was purchased from Tokyo Chemical Industry Co. Ltd. Japan. The 50 wt % aqueous NMMO solution (approximately 4.8 mol/L) was condensed to NMMO 0.9 hydrate in an evaporator with a vacuum at 120°C.

Preparation of spinning solution

The spinning solution was prepared by taking 40 mL NMMO 0.9 hydrate (solvent), 4 g bagasse (cellulose), 10 mg propyl gallate (antioxidant), and 10 mg sodium dodecyl-sulfate (surfactant) in a flask and stirring the solution in a static rotary mixer at 50 rpm at 120°C for 2.5 h.

Dry jet-wet spinning

Dry jet-wet spinning was carried out at 100°C with an air gap of 10∼ 15 mm through a single-hole spinneret of diameter 0.5 mm. The injection speed was approximately 4.0 m min^{-1}. Coagulation took place in aqueous NMMO solutions containing NMMO concentrations 0%, 2%, 5%, 10%, 20%, 30%, 40%, and 50 wt % at room temperature (20°C) with a 2-m coagulating bath followed by a water wash.

The prepared fibers were taken up at their maximum possible speeds, which ranged between 19 and 64 m min^{-1}. The spin-draw ratio (v_f/v_0) was determined by measuring the cross-sectional diameter of the solution dope in the spinneret exit. Here, v_f is the take-up velocity of the prepared fiber and v_0 is the extrusion velocity at the spinneret.

Spun fibers were dried in an oven at 30°C for 24 h in the presence of silica gel to absorb water.

Measurements

Structural characterization

Birefringence was conducted by measuring the refractive indices parallel and perpendicular to the fiber axis by an Interphako Interference Microscope (Carl Zeiss JENA Ltd., Germany). During each measurement, five fiber specimens were taken from five different positions and then averaged.

Wide-angle X-ray diffraction (WAXD) measurements were obtained by a Rigaku Rotorflex RU-200B diffractometer using Ni-filtered Cu-K_α radiation operated at 40 kV and 150 mA (wavelength 1.542 Å). The degree of crystallinity was determined from the ratio of crystalline scattering versus total scattering, whereby the amorphous contribution was estimated by polynomial approximation.[25] The angle of preferred orientation with respect to the fiber axis was determined from the most intense reflection peak of equatorial diffraction (with an overlapping 110/200 plane at $2\theta = 22.6°$).[26,27] Curves derived from the azimuthal scans were fitted to the profiles of the mathematical model using Gauss functions,[28] as shown in eq. (1), where I_o is the peak intensity, ϕ_0 is the azimuthal angle at I_o, and τ is the peak width. Herman's crystal orientation functions, f_c, were then obtained with eq. (2):

$$I_{(\phi)} = I_o \exp\left\{-\left(\frac{\phi - \phi_o}{\tau}\right)^2\right\} \quad (1)$$

$$f_c = \frac{3\langle\cos^2\phi\rangle - 1}{2} \quad (2)$$

where

$$\langle\cos^2\phi\rangle = \frac{\int_0^{\pi/2} I_{(\phi)} \cos^2 \sin\phi d\phi}{\int_0^{\pi/2} I_{(\phi)} \sin\phi d\phi}$$

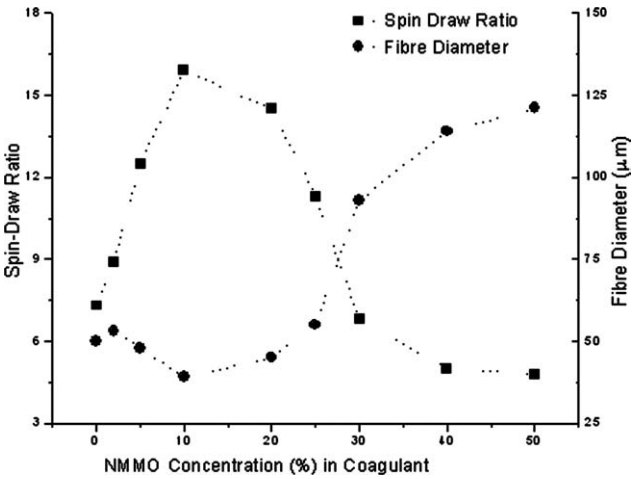

Figure 1 Spin-draw ratio versus diameter of lyocell fibers as a function of NMMO concentration in the coagulating bath.

Scanning electron microscopy (SEM) was conducted with a Hitachi *S*-2380*N* after sputtering the samples with platinum (Pt).

DSC analyses were performed on a Perkin–Elmer Pyris-1 analyzer. Both temperature and heat flow were calibrated with the standard indium reference. Fiber weights were maintained within the range of 2 $\sim$ 3 mg. All thermal analyses were carried out under a dry nitrogen atmosphere.

TGA was accomplished with the ThermoPlus II TG-DTA 8120 from room temperature to 600°C in air at a scan rate of 10°C min^{-1}. The weight of each sample was 5 mg.

FTIR measurements were performed by means of FTIR-8600PC (Shimazu Ltd., Japan).

Fibrillation of the fibers was achieved by taking 10 fibers of 20 mm length. Fibers were immersed in distilled water at room temperature (20°C) and sonicated for 15 min on a Branson ultrasonic sonifier 2510 OJ-DTH.[29]

Mechanical properties

The tensile properties of lyocell fibers (40 mm gauge length) were measured in Tensilon Model RTC-1250A (Japan) with a 10*N* load cell at a crosshead speed of 40 mm min^{-1}. The experimental results represent the average of 10 individual measurements.

Dynamic mechanical properties

The dynamic viscoelastic properties were measured by an ITK Co. DVA-225 instrument at a frequency of 10 Hz and a heating rate of 10°C min^{-1} on fibers of 20 mm length.

RESULTS AND DISCUSSION

Appearance of lyocell fibers

The physical appearance of the lyocell fibers prepared from bagasse was visually observed. All fibers' exterior showed the silky luster like commercial lyocell fibers irrespective of the NMMO concentration in the coagulating bath.

Structure development

The spin-draw ratio and resultant diameters of lyocell fibers obtained in water/NMMO coagulants of different NMMO concentrations are illustrated in Figure 1. As shown, the spin-draw ratio of fibers increases to its highest value, 16 times, as the NMMO concentration increases to 10%, and then decreases as the NMMO concentrations increase to 50%. The fiber diameter decreases to 38 μm for the water/NMMO (10%) coagulant and then again increases to 122 μm as the spin-draw ratio decreases and the water/NMMO concentration increases to 50%. At NMMO concentrations of 30% or higher, there is a sudden decrease in the spin-draw ratio and an increase in fiber diameter.

In Figures 2 and 3, the birefringence and crystallinity/crystal orientation of the prepared fibers, respectively, are shown as a function of the NMMO concentration in the coagulating bath. In general, structural parameters of the fibers such as birefringence, crystallinity, and crystal orientation change according to the draw ratio. As shown in Figures 2 and 3, the tendency of the changing birefringence and crystal orientation with draw ratio are very plausible, and the values are the highest for fiber from the water/NMMO (10%) coagulant. But the crystallinity of the fibers with NMMO concentrations 5%, 10, and 20% are lower than their expected

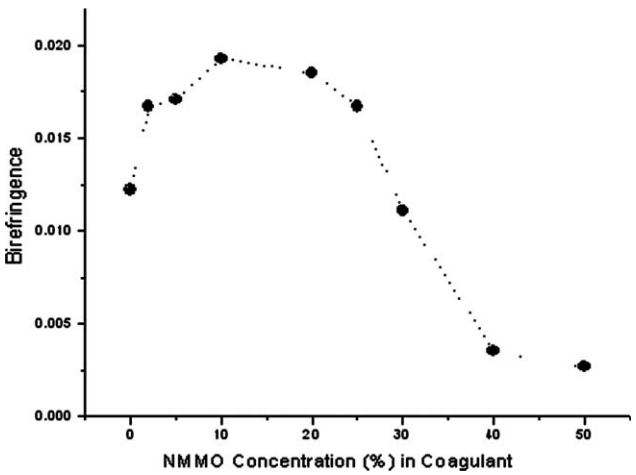

Figure 2 Birefringence as a function of NMMO concentration in coagulating bath.

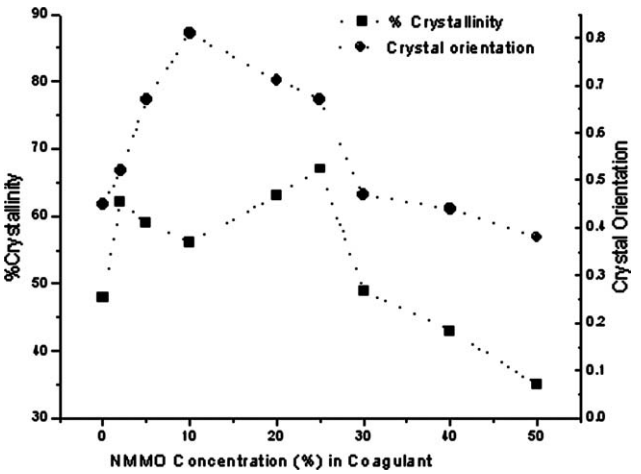

Figure 3 Crystallinity and crystal orientation factor as a function of NMMO concentration in the coagulating bath.

values. The reason for this was thought to be the NMMO solvent remaining in the fiber matrix; this condition was investigated and later confirmed by FTIR measurement.

The crystallinity and crystal orientation can also be qualitatively compared by WAXD patterns, shown in Figure 4, which shows that the crystal order improves with increasing spin-draw ratio and is highest for the NMMO (10%) coagulant fibers. The broadening of equatorial spots in the case of 5%, 10, and 20% NMMO coagulant fibers indicates their lower crystallinity in comparison with that of the 2 and 25% NMMO coagulant fibers. But the broadening of X-ray spots in the azimuthal direction becomes narrower with the increase of the draw ratio, and the NMMO (10%) fiber shows the sharpest azimuthal spot, that is, the highest crystal

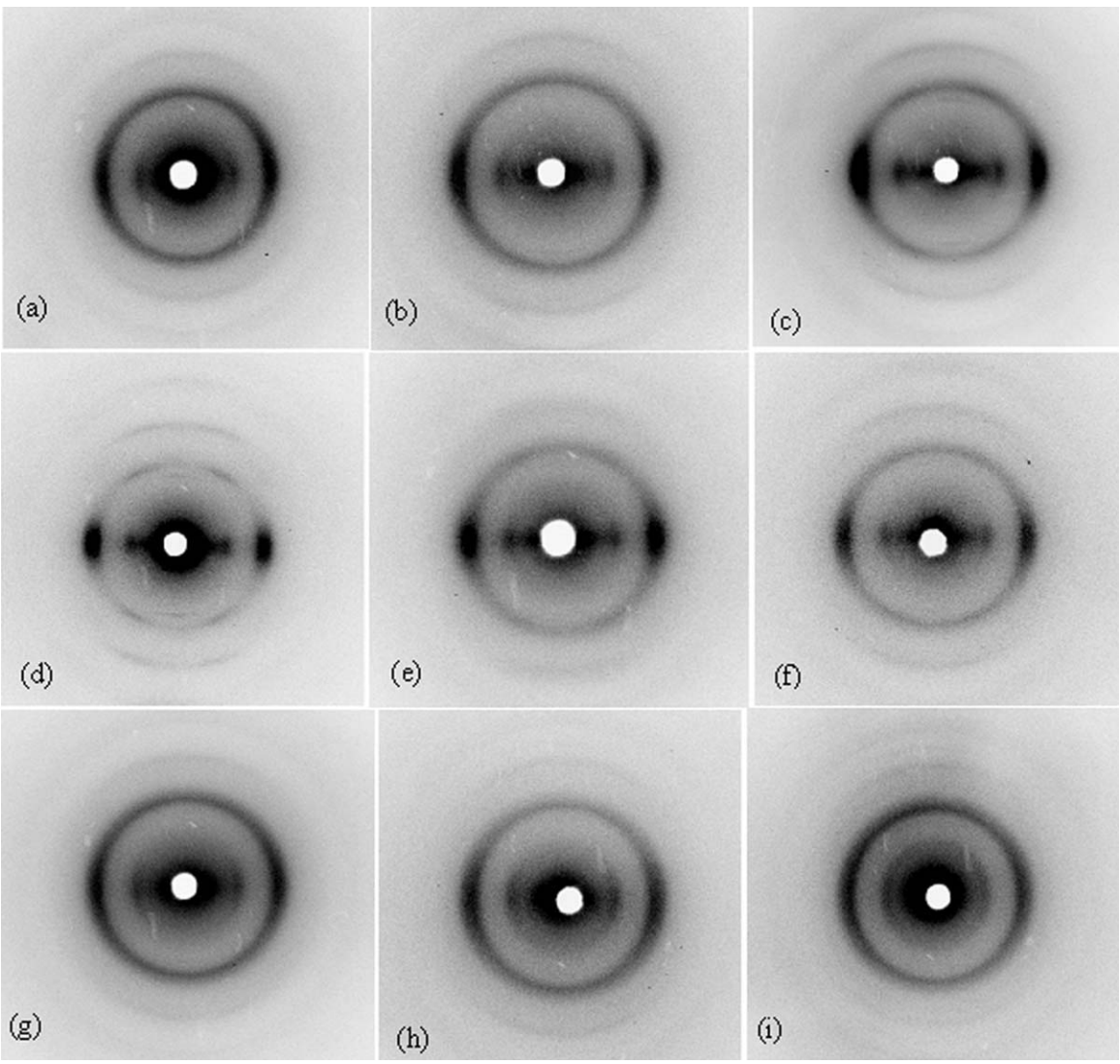

Figure 4 WAXD images of lyocell fibers obtained in various water/NMMO concentrations. (a) Water only, (b) NMMO 2%, (c) NMMO 5%, (d) NMMO 10%, (e) NMMO 20%, (f) NMMO 25%, (g) NMMO 30%, (h) NMMO 40%, and (i) NMMO 50%.

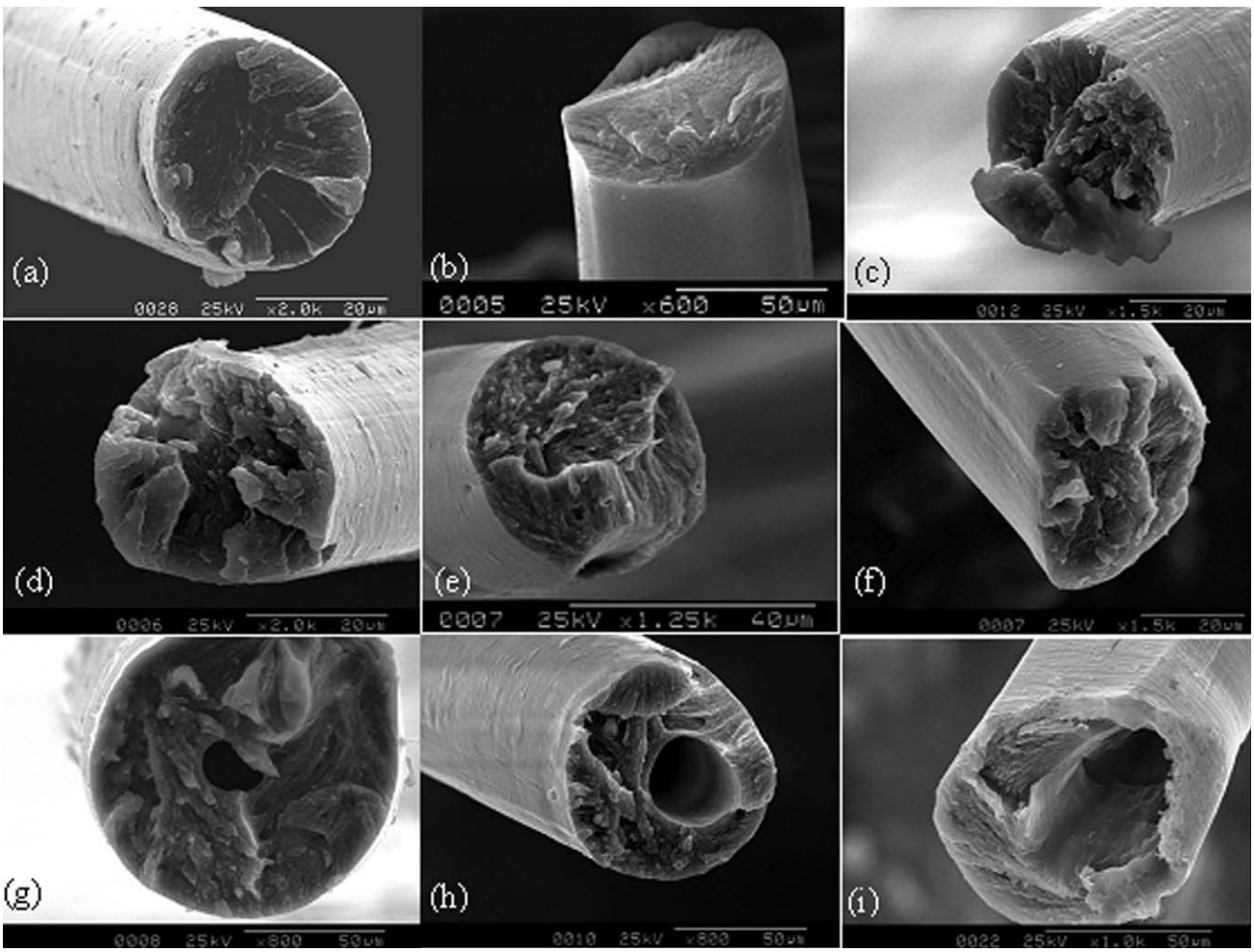

Figure 5 SEM images of fractured cross-sections of lyocell fibers for various water/NMMO concentrations. (a) Water only, (b) NMMO 2%, (c) NMMO 5%, (d) NMMO 10%, (e) NMMO 20%, (f) NMMO 25%, (g) NMMO 30%, (h) NMMO 40%, and (i) NMMO 50%.

orientation. This agrees well with the values of crystal orientation plotted in Figure 3. As indicated by numerous studies of birefringence and X-rays, a compact structure, as a rule, has a higher orientation and higher crystalline order. Here, NMMO (10%) coagulant fiber shows the highest compactness, that is, the lowest diameter, 38 μm, among all coagulant fibers.

The morphological structure of fibers was studied by observing fractured cross-sections of fibers in SEM, as presented in Figure 5. Because NMMO is a strongly hygroscopic substance,[30] the only water and NMMO (2%) coagulant fibers seemed to be instantly coagulated immediately after entering the water-predominant coagulating baths. This reason might lead to the lower spin-draw ratios and lower structural parameters of these fibers. The fibers obtained from the baths of water/NMMO concentrations 5%, 10%, 20, and 25% show some indication of fibrillation. The occurrence of fibrillation of lyocell fibers is attributed to their high birefringence, crystallinity, and crystal orientation caused by the high spin-draw ratio. One interesting outcome of this study is the formation of hollow lyocell fibers when fibers were coagulated in water/NMMO solution containing 30% NMMO and higher. It is thought that these fibers could not coagulate in the coagulating bath due to higher NMMO concentrations (30 to 50%) but coagulated very rapidly in the wash bath containing water. During such rapid coagulation, a longitudinal void or hollow at the fiber center is created. Another point worth noting is that the size of the hollow center can be controlled because it becomes gradually larger with the increase of NMMO concentration from 30 to 40% to 50%. Such hollow lyocell fibers are assumed to be highly hygroscopic in nature and thus advantageous in apparel or filtration materials with high absorbability.

Correlation of mechanical properties with fiber structure

Figure 6 shows typical stress-strain curves of the fibers obtained in the various NMMO concentrations

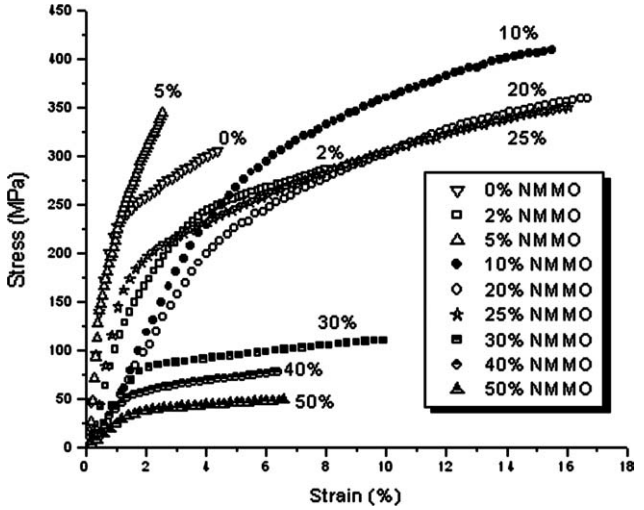

Figure 6 Stress-strain curves of lyocell fibers prepared in various water/NMMO concentrations.

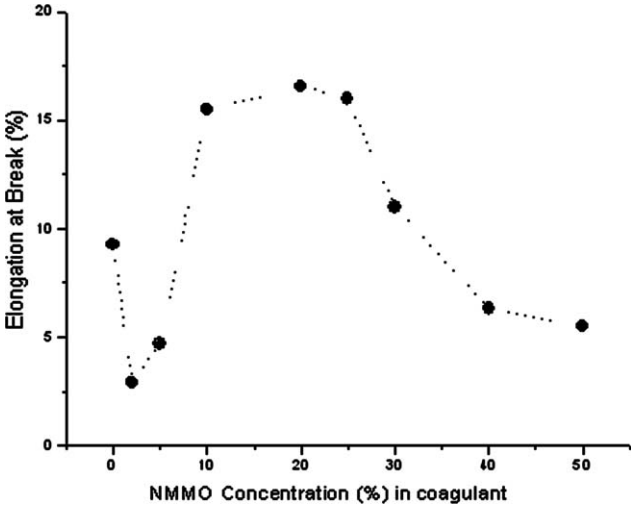

Figure 8 Elongation at break (%) of lyocell fibers prepared in various water/NMMO concentrations.

of coagulants. At a glance, the tensile properties of the fibers obtained in NMMO 0 (water only), 2, and 5% coagulants are somewhat similar. Tensile strength with toughness improves markedly for fibers coagulated in 10, 20, and 25% NMMO solutions. The lowest tensile properties are observed for the fibers coagulated in highly concentrated NMMO solutions, such as 30, 40, and 50%.

Tensile strength and initial modulus, and elongation at the break, as evaluated from the stress-strain curves, are shown in Figures 7 and 8, respectively. As is generally known, the tensile strength of a fiber is determined by the degree of chain extension and the degree of overall molecular orientation relative to the fiber axis.[31] By referring back to the birefringence and crystal orientation data in Figures 2 and 3, a strong correlation between tensile strength and these structural parameters can be found. As shown in Figure 7, the initial modulus of the fibers obtained in 5, 10, and 20% NMMO baths does not follow the same increasing trend of tensile strength: instead, they show a lower modulus. The tendency of the initial modulus with the NMMO concentration seems to correspond to the level of crystallinity shown in Figure 3. It is well known that the initial modulus of the fiber is a function of both crystallinity and molecular orientation.[32] Consequently, the modulus of lyocell fibers prepared in this study could be governed by their crystallinity. However, the reason for the low crystallinity and low modulus for fibers obtained in the baths of 5, 10, and 20% NMMO concentrations was previously speculated to be due to the remaining NMMO in the fiber matrix. Not surprisingly, the hollow fibers obtained in the baths of

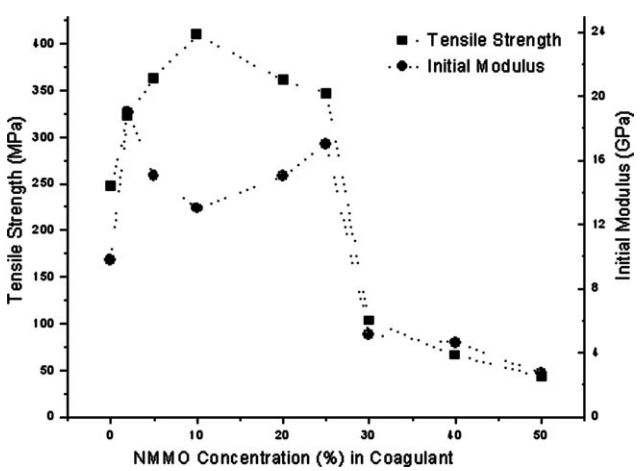

Figure 7 Tensile strength and initial modulus of lyocell fibers prepared in various water/NMMO concentrations.

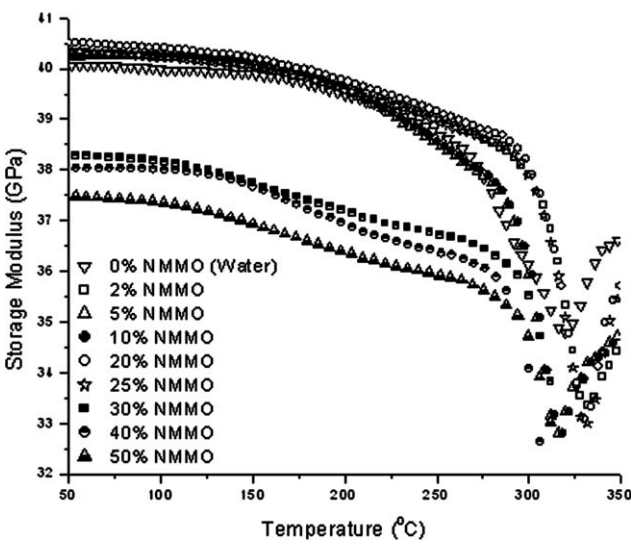

Figure 9 Storage modulus (E') of lyocell fibers prepared in various water/NMMO concentrations.

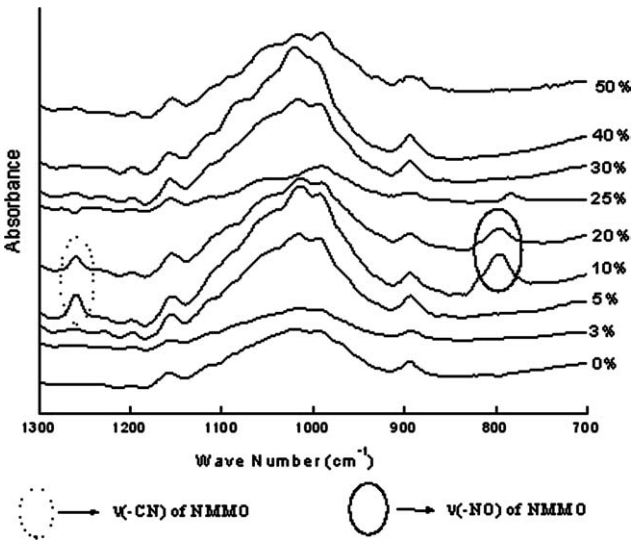

Figure 10 FTIR curves of lyocell fibers prepared in various water/NMMO concentrations.

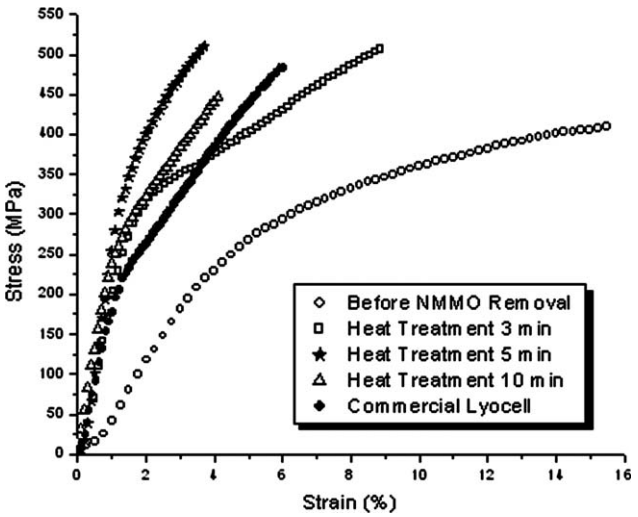

Figure 12 Stress-strain curves before and after elimination of NMMO of water/NMMO (10%) coagulated lyocell fibers in comparison with commercial lyocell fiber.

30, 40, and 50% NMMO concentrations show the lowest tensile properties.

Figure 8 shows the breaking elongations of all fibers. Among these fibers, the elongation at break is higher for the fibers prepared in the 10, 20, and 25% NMMO baths. The NMMO remaining in the fiber matrix on the elongation at the break of these fibers is assumed to be an influence.

The temperature dependence in the mechanical properties of the fibers is next investigated by the dynamic viscoelastic analysis. In Figure 9, the storage modulus (E') of all fibers is demonstrated. The fiber at the NMMO (10%) concentration does not show the highest E' values across the entire temperature range due to the remaining NMMO. As seen in the tensile properties, hollow fibers have the lowest E' values.

From the above discussion, it can be concluded that the highest drawn fiber obtained from the NMMO (10%) coagulant attained superior structural features and mechanical properties, even though the NMMO remaining leads to lower crystallinity and tensile strength than their actual values.

It is likely that the coagulants containing low NMMO concentrations, such as 0 (water only), 3, and 5%, act as very fast coagulants because the water percentage is so high. Conversely, the coagulants containing high NMMO concentrations, such as 30, 40, and 50%, act as very slow coagulants because the NMMO percentage is very high. The coagulants containing intermediate NMMO concentrations, 10, 20, and 25%, seem to show coagulation more favorably than the very low and very high NMMO concentrations. Of the 10, 20, and 30%

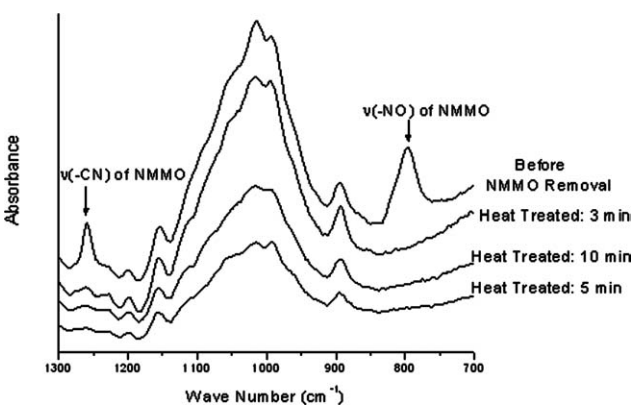

Figure 11 FTIR curves of water/NMMO (10%) lyocell fiber to observe the elimination of NMMO after heat treatment.

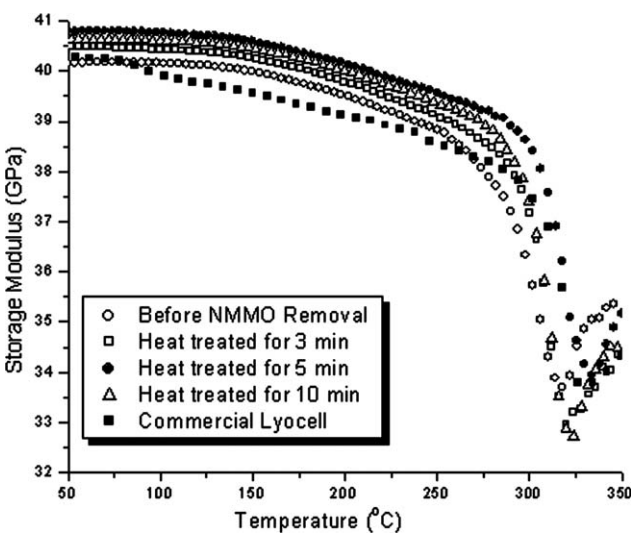

Figure 13 Storage modulus before and after elimination of NMMO of water/NMMO (10%) coagulated lyocell fibers in comparison with commercial lyocell fiber.

TABLE I
Structure and Mechanical Properties of Lyocell Fibres Prepared in Water/NMMO (10%) after NMMO Removal by Heat Treatment

Heat treatment time	Tensile strength (MPa)	Initial modulus (GPa)	Elongation at break (%)	Degree of crystallinity, x_c (%)	Degree of crystal orientation (f_c)	Birefringence (Δn) $\times 10^3$
Before heat treatment	410	13	15	56	0.81	19.3
3 min	493	24	6.8	65	0.83	22.8
5 min	510	30	5.4	71	0.86	23.2
10 min	429	20	4.6	68	0.79	20.8

NMMO concentrations, the 10% NMMO mixture seems to meet the requirement for optimal coagulation.

NMMO removal from the fiber matrix

The remaining NMMO in all prepared fibers was investigated by FTIR spectra. As shown in Figure 10, stretching bands appear at approximately 1260 and 800 cm^{-1}, corresponding with ν(—CN) and ν(—NO) stretching of NMMO, respectively, for coagulant fibers of 10 and 20% NMMO. This finding confirmed the low crystallinity and modulus values of these fibers. However, to evaporate NMMO from inside the fibers, the fibers were subjected to heat treatment at 250°C, where E' of these fibers (Fig. 9) begins to drop. However, the fibers were heat treated at 250°C with tension for various period of time of 3, 5, and 10 min and their physical properties were measured. Figure 11 shows the FTIR spectra for NMMO (10%) fibers before and after NMMO evaporation. The IR bands of 1260 and 800 cm^{-1} disappear, even after heat treating for 3 min, suggesting the evaporation of NMMO from the fibers.

Characteristics of fibers after NMMO removal

In the above discussion, the NMMO (10%) fiber showed the most promising physical properties. Thus, we again investigated the structure and mechanical properties of this fiber after NMMO removal.

Stress-strain curves of NMMO (10%) fiber before and after NMMO removal, together with the curve of commercial lyocell fiber, are illustrated in Figure 12. As shown by the stress-strain curves, the overall tensile properties of fibers remarkably improved after NMMO removal by heat treatment. Specifically, the shape of the stress-strain curves becomes gradually steeper after heat treatment for 3 and 5 min but declines with the further treatment time of 10 min may be due to the disordering crystallites with the high temperature of heat treatment. Hence, the treatment time of 5 min was considered to be the optimum in terms of physical properties.

The storage modulus curves (E') of heat-treated NMMO (10%) fibers are shown in Figure 13. The E' values of fiber noticeably increase across the entire temperature range after NMMO removal, irrespective of the treatment time. The sample heat treated for 5 min sample shows the highest E' as well as the maximum value ($\sim$ 41 GPa) at room temperature (20°C). The increase in E' value for the sample heat treated for 5 min suggests the highest level of molecular orientation and crystallinity for NMMO (10%) heat-treated fiber.

Table I lists the structural parameters and mechanical properties of NMMO (10%) fibers after NMMO

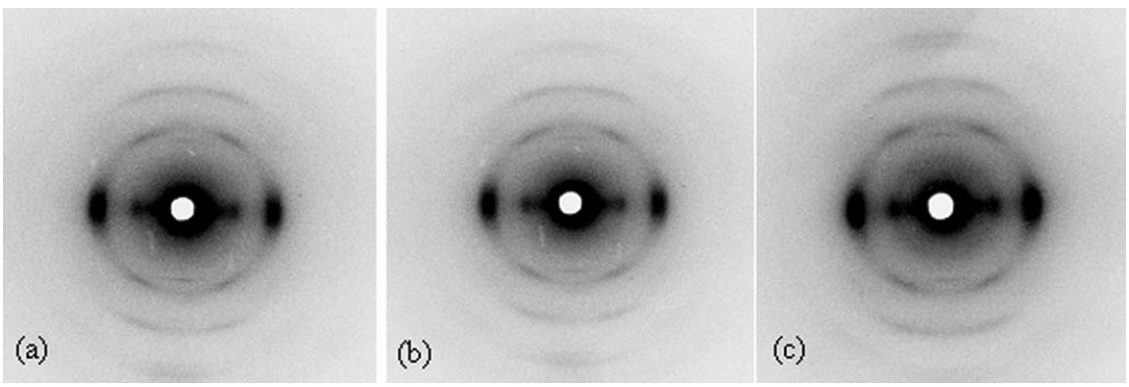

Figure 14 WAXD images of water/NMMO (10%) coagulated lyocell fibers after NMMO removal by heat treatment for (a) 3 min, (b) 5 min, and (c) 10 min.

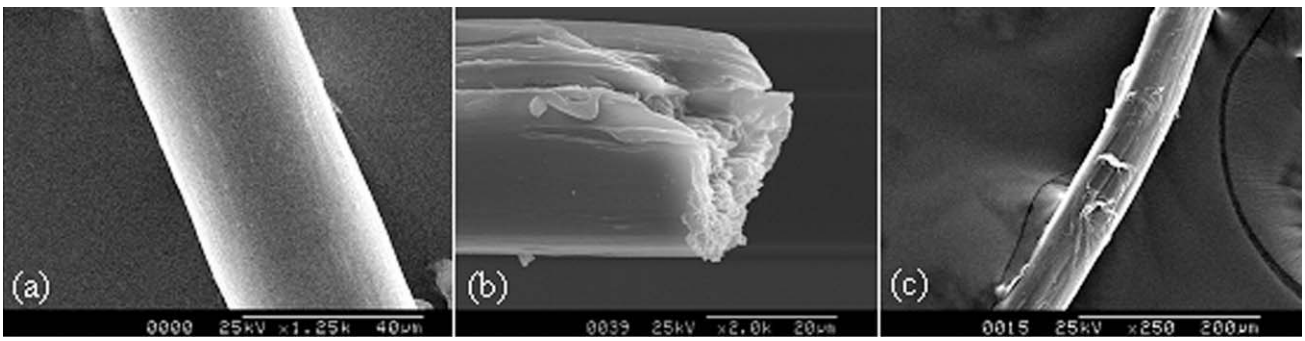

Figure 15 SEM images of water/NMMO (10%) coagulated lyocell fibers after NMMO removal by heat treatment for 5 min: (a) surface (b) cross-section, and (c) surface after sonication.

removal for different heat-treatment times. The improvements in the structure of fibers have a strong correlation with their respective tensile properties. As shown, after NMMO removal, the fibers exhibit increased molecular structures, such as crystallinity, crystal orientation, and birefringence, which result in significant enhancement in mechanical properties and a reduction in the elongation at break. WAXD images of these fibers, shown in Figure 14, also clearly indicate the improvement in crystallinity and crystal orientation after NMMO removal. Among the three treated samples, the sample heat treated for 5 min shows the sharpest crystal spots. In Figure 15, SEM images of the 5-min-treated fiber provide clear information about its smooth fiber surface and the occurrence of fibrillation. This fibrillation phenomenon can be attributed to its high degree of crystallinity and high orientation of the molecular chains in the noncrystalline regions of the fiber.[33,34]

In this work, tensile strength of 510 MPa and initial modulus of 30 GPa are reported for lyocell fibers prepared from bagasse. These results are comparable with the results of the commercial lyocell fiber used in our study (tensile strength 486 MPa and initial modulus 16 GPa), and the results reported in related literature (tensile strength 525 $\sim$ 600 MPa, and initial modulus 8 $\sim$ 18 GPa).[35,36]

CONCLUSIONS

Sugarcane bagasse was dissolved in NMMO 0.9 hydrate, and fibers were prepared by dry jet-wet spinning in aqueous NMMO solutions. We evaluated different NMMO concentrations from 0 to 50% in aqueous coagulating baths. Of these solutions, fibers prepared in water/NMMO (10%) show the overall highest physical properties. The spun fibers prepared in water/NMMO (10%) coagulant contain remaining solvent NMMO in the fiber matrix that can be removed by a simple heat treatment. After removal of NMMO by heating, much improvement in fiber structure and material properties is found. The exterior appearance of these fibers is smooth and very shiny.

The overall properties of the lyocell fibers prepared from bagasse are very comparable with those of commercial lyocell fibers. Thus, it can be concluded that sugarcane bagasse is a very cheap source of raw material for producing lyocell fibers of commercial grade.

References

1. Ikeda, Y.; Tsuji, H. Macromol Rapid Commun 2000, 21, 117.
2. Kanie, O.; Tanaka, A.; Mayumi, T.; Kitaoka, T.; Wariishi, H. J Appl Polym Sci 2005, 96, 861.
3. Franks, N. E.; Varga, J. K.; (to Akzona Inc.). US Pat. 4,145,532 (1979).
4. McCorseley, C. C., III; Varga, J. K.; US. Pat. 4,142,913 (1979).
5. Chanzy, H.; Peguy, S.; Chaunis, S.; Monzie, P. J Polym Sci Part B: Polym Phys 1980, 18, 1137.
6. Woodings, C. R. Int J Biol Macromol 1995, 17, 305.
7. Federal Trade Commission, FTC File No. P92-8401 (1992).
8. Loubinoux, D.; Chaunis, S. Textile Res J 1987, 57, 61.
9. Colom, X.; Carrillo, F. Eur Polym Mater 2002, 38, 2225.
10. Gindl, W.; Keckes, J. Compos Sci Tech 2006, 2049, 66.
11. Kim, D. B.; Pak, J. J.; Jo, S. M.; Lee, W. S. Textile Res J 2005, 75, 331.
12. Mortimer, S. A.; Péguy, A. A. J. Appl Polym Sci 1996, 60, 305.
13. Huiru, R. Z; Liu, X; Li, D; Li, R. J Appl Polym Sci 2009, 113, 150.
14. Chiparus, O. L. PhD Thesis, Louisiana State University, 2004.
15. Luo, M. K.; Rosceli, V. A.; Sealey, J.; Neogi, A. N. Presented at the 5th International Symposium, April 5, 2002, Rudolstadt, Germany.
16. Huiru, R.; Mingwei, T. Polym Eng Sci 2007, 47, 702.
17. Huiru, Z.; Huihui, Z.; Mingwei, T.; Huili, S.; Xuechao, H. J Appl Polym Sci 2008, 107, 636.
18. Hult, E.-L.; Larsson, P. T.; Iversen, T. Polymer 2001, 42, 3309.
19. Hult, E.-L.; Larsson, P. T.; Iversen, T. Cellulose 2000, 7, 35.
20. Newman, R. H. Solid State Nucl Magn Reson 1999, 15, 21.
21. Hult, E.-L.; Larsson, P. T.; Iversen, T. Cellulose 2001, 8, 209.
22. Atalla, R. H.; Hackney, J. M.; Uhlin, I; Thompson, N. S. Int J Biol Macromol 1993, 15, 109.
23. Lenz, J; Schurz, J; Wrentschur, E. Colloid Polym Sci 1993, 271, 460.
24. Lenz, J; Schurz, J; Wrentschur, E. J Appl Polym Sci 1987 1988, 35.

25. Smole, M. S.; Persin, Z.; Kreze, T.; Kleinschek, K. S.; Ribitsch, V.; Neumayer, S. Mater Res Innovat 2003, 7, 275.
26. Gindl, W.; Keckes, J. Compos Sci Tech 2006, 2049, 66.
27. Fink, H.-P.; Weigel, P.; Purz, H. J.; Ganster, J. Prog Polym Sci 2001, 26, 1473.
28. Heuvel, H. M.; Huisman, R.; Lind, K. C. J. B. J Polym Sci Part B: Polym Phys 1976, 14, 921.
29. Kim, D. B.; Lee, W. S.; Kim, B. C.; Jo, S. M.; Park, J. S.; Lee, Y. M. Polymer Kor 1998, 22, 231.
30. Hall, M. E.; Horrocks, A. R.; Seddon, H. Polym Degrad Stab 1999, 64, 505.
31. Suzuki, A.; Murata, H.; Kunugi, T. Polymer 1997, 39, 1351.
32. Mezghani, K.; Spruiell, JE. J Polym Sci Part B: Polym Phys 1998, 36, 1005.
33. Kreze, T.; Malej, S. Textile Res J 2003, 73, 675.
34. Lenz, J; Schurz, J; Wrentschur, E. Acta Polym 1992, 43, 307.
35. Ibbett, R. N.; Hsieh, Y. L. Textile Res J 2001, 71, 164.
36. Perepelkin, K. E. Fibre Chem 2007, 39, 163.